Journal of Inflammation Research

Dovepress
Taylor & Francis Group

Open Access Full Text Article

ORIGINAL RESEARCH

# Combination of Polydatin and Hawthorn Leave Flavonoids Ameliorate Atherosclerotic Plaque Vulnerability in ApoE$^{-/-}$ Mice by Regulating Ferroptosis via the Nrf2/HO-1/GPX4 Axis

Jiye Chen[1,2,*], Xiaonan Zhang[1,*], Changxin Sun[1,3,*], Zeping Wang[1], Xiaoya Li[1], Lanqing Hu[1], Yongfang Yuan[1], Min Wu[4], Longtao Liu[1]

[1]State Key Laboratory of Traditional Chinese Medicine Syndrome/National Clinical Research Center for Chinese Medicine Cardiology, Xiyuan Hospital, China Academy of Chinese Medical Science, Beijing, 100091, People's Republic of China; [2]Department of Cardiovascular, Affiliated Hospital of Shandong University of Traditional Chinese Medicine, Shandong, 250014, People's Republic of China; [3]Graduate School, Beijing University of Chinese Medicine, Beijing, 100029, People's Republic of China; [4]Department of Cardiovascular, Guang'an Men Hospital, China Academy of Chinese Medical Sciences, Beijing, 100053, People's Republic of China

*These authors contributed equally to this work

Correspondence: Longtao Liu; Min Wu, Email liulongtao1976@126.com; wumin19762000@126.com



**Background:** Atherosclerosis (AS) is a chronic inflammatory vascular disease in which ferroptosis plays a crucial role. While the combination of polydatin (PD) and Hawthorn leaf flavonoids (HLF), termed PD and HLF combination (PH), is effective against AS, its impact on plaque vulnerability and the underlying mechanisms remain unclear.

**Methods:** ApoE$^{-/-}$ mice were fed a high-fat diet (HFD) for 12 weeks to establish an AS model and treated with PD, HLF and Simvastatin for 8 weeks. Histological characterization of atherosclerotic lesions was performed using pathological staining. Transmission electron microscopy (TEM) was used to evaluate mitochondrial damage. Lipid peroxidation levels were assessed using ELISA. Immunofluorescence staining was performed to verify Nrf2 nuclear translocation. Expression of the Nrf2/HO-1/GPX4 axis was detected using Western blotting and PCR.

**Results:** HFD significantly promoted AS lesion formation and instability, and caused severe iron overload and lipid peroxidation in atherosclerotic lesions. PH significantly reduced dyslipidemia and suppressed atherosclerotic plaque progression in ApoE-/- mice. Meanwhile, the PH combination visibly reduced iron accumulation and improved mitochondrial ultrastructure. Additionally, PH combination decreased the levels of ROS, MDA, 4HNE, 8-OHdG, and $Fe^{2+}$, while increasing GSH levels. Further studies showed that the PH combination enhanced the translocation of Nrf2 into the nucleus, HO-1, GPX4, SLC7A11, FPN1, and FTH1 expression, and inhibited cytoplasmic Nrf2 and TFR1 expression.

**Conclusion:** PH combination reduced the instability of atherosclerotic lesions in ApoE$^{-/-}$ mice by modulating iron metabolism and lipid peroxidation through activation of the Nrf2/ HO-1/GPX4 axis.

**Keywords:** atherosclerotic plaque vulnerability, ferroptosis, Nrf2/ HO-1/GPX4 axis, polydatin, hawthorn leave flavonoids

## Introduction

Atherosclerosis (AS) is a chronic inflammatory vascular disease characterized by abnormal lipid metabolism and inflammatory responses in the arterial wall caused by endothelial injury.[1] During AS development, substantial lipid deposition and the formation of necrotic cores cause the formation of vulnerable plaques.[2] Plaque rupture and secondary thrombus formation are the major pathological bases of myocardial infarction, stroke, and other atherosclerotic cardiovascular disease (ASCVD) complications. Increasing epidemiological studies have shown that AS is the leading contributor of global morbidity and mortality.[3,4] Therefore, the pathogenesis and treatment of AS are important areas of medical research in ASCVD. Clinically,

Received: 28 March 2025
Accepted: 13 August 2025
Published: 2 September 2025

lipid-lowering and antiplatelet therapies are the main medications used for AS management; however, these interventions cannot effectively reduce adverse cardiovascular events.[5] Consequently, clarifying the pathological mechanisms and exploring effective therapies have become the focus of clinical studies on AS.

Although atherosclerotic plaque stability is mediated by many complicated pathological processes, cell death is a pivotal pathological process in its etiology and progression.[6] Multiple studies have confirmed that cell death plays a vital role in the instability and rupture of atherosclerotic plaques.[7,8] Ferroptosis is a non-apoptotic type of programmed death involving intracellular iron overload and aberrant accumulation of lipid peroxides.[9,10] Ferroptosis exacerbates the risk of unstable plaque shedding through dysregulated iron metabolism and lipid peroxidation, primarily mediated by plaque cells. Endothelial cell ferroptosis compromises vascular barrier integrity and enhances monocyte adhesion,[11] while macrophage ferroptosis amplifies foam cell formation and necrotic core expansion through erythrophagocytosis-induced iron overload.[12] Concurrently, vascular smooth muscle cell ferroptosis drives synthetic phenotype switching.[13] These pathological processes are mechanistically underpinned by iron-dependent Fenton reactions that generate cytotoxic lipid peroxides, synergistically coupled with the collapse of the solute carrier family 7 member 11 (SLC7A11)/glutathione (GSH)/glutathione peroxidase 4 (GPX4) antioxidant axis, which impairs lipid peroxide detoxification. Consequently, therapeutic inhibition of ferroptosis attenuates atherogenic lipid deposition and stabilizes vulnerable plaques.[14] Inhibition of ferroptosis can improve lipid deposition and formation of a necrotic core in AS.[15] Therefore, the attenuation of ferroptosis may represent a novel strategy for the treatment of AS.[12]

Nuclear factor erythroid 2-related factor 2 (Nrf2) is a major transcription factor that plays a pivotal role in the cellular redox balance.[16] Under physiological conditions, Nrf2 forms a complex with Keap1, leading to its proteasomal degradation. Oxidative stress can lead to the dissociation of Keap1 from Nrf2, its subsequent transfer into the nucleus, and its interaction with HO-1 to initiate the transcription of downstream targets.[17] Nrf2 activation regulates the expression of GPX4 and SLC7A11, which are involved in the regulation of oxidative stress.[18] Furthermore, Nrf2 regulates the expression of iron metabolism proteins, such as ferritin heavy chain 1 (FTH1), ferroportin 1 (FPN1), and transferrin receptor protein 1 (TFR1),[19] thereby modulating ferroptosis. Therefore, the activation of the Nrf2/HO-1/GPX4 axis has been speculated to mitigate ferroptosis by regulating iron homeostasis and lipid peroxidation.[20]

In recent years, the importance of the active ingredients of Chinese medicines in the prevention and treatment of AS has attracted extensive attention from scientists.[21] Polydatin (PD) is the main component of Polygonum cuspidatum and possesses a variety of pharmacological effects, such as anti-inflammatory properties and endothelial protection activity.[22] Our previous study suggested that PD suppresses atherosclerotic plaque formation by regulating the nucleotide-oligomerization (NOD)-like receptor (NLR) family pyrin domain-containing protein 3 (NLRP3)/mammalian target of rapamycin (mTOR) pathway.[23] PD also decelerated AS progression by inhibiting oxidized low-density lipoprotein (ox-LDL)-induced foam cell formation in murine macrophages.[24] Hawthorn leaf flavonoids (HLF), which are the main components of Hawthorn extract, have antioxidant and lipid-modulatory effects in AS.[25] Our previous animal experiments showed that HLF could reinforce plaque stability by suppressing the inflammatory response and apoptosis.[26] Our randomized controlled clinical trial found that the combination of Polygonum cuspidatum and Hawthorn could help reduce angina symptoms in patients with unstable angina and improve prognosis and inflammation-related indicators.[27] Our previous network pharmacology study showed that the combination of Polygonum cuspidatum and hawthorn could alleviate coronary heart disease by regulating lipid metabolism and inflammation.[28] However, the effect of the combination of PD and HLF combination (PH) on plaque stability and its molecular mechanisms remain unclear.

In this study, we aimed to investigate the therapeutic effects and fundamental mechanisms of PH combination therapy on plaque stability. We hypothesized that PH combination may attenuate AS lesion formation and instability by suppressing ferroptosis via the activation of the Nrf2/HO-1/GPX4 axis. To test this hypothesis, we simulated the AS model using an in vivo experiment.

# Materials and Methods

## Chemicals Drugs

PD (purity ≥ 98%) was obtained from Shanxi Guanjie Biotechnology Co., Ltd. (Shanxi, China; PO210425). HLF was purchased from Shandong Linyi Aikang Pharmaceutical Co. Ltd. (Shandong, China; AKH15-2). Simvastatin (SVT) was acquired from Hangzhou MSD Pharmaceutical Co. Ltd. (Hangzhou, China; U010049).

## Animal Models and Intervention

Male C57BL/6J and ApoE$^{-/-}$ mice aged 8 weeks were acquired from Spareford Biotechnology Co., Ltd. (SCXK [Beijing] 2019-0010). The mice were housed in the animal facility at Xiyuan Hospital, with access to tap water, under a 12-hour light/dark cycle, in an environment with a constant temperature of 22±2 °C and 55 ± 5% relative humidity. The mice underwent a 7-day acclimatization period during. Following acclimatization, all ApoE$^{-/-}$ mice were assigned unique identification codes and randomly allocated using a computer-generated randomization sequence by an independent researcher. In accordance with the experimental protocol, C57BL/6J mice were allocated to a normal diet (ND) group, which received a standard diet, whereas ApoE$^{-/-}$ mice were randomly distributed among five treatment groups: high-fat diet (HFD), PD (PD 200 mg/kg/day), HLF (HLF 100 mg/kg/day), PH (PD 200 mg/kg/day and HLF 100 mg/kg/day), and simvastatin (SVT) (SVT 5 mg/kg). To induce AS, all ApoE$^{-/-}$ mice were maintained on a HFD for 12 weeks, followed by an 8-week oral gavage treatment. Drug solutions were prepared daily by a technician not involved in behavioral or histological analyses, and administered blindly using coded syringes. The body weight of the mice was monitored weekly. After 20 weeks, all animals were anesthetized with isoflurane and measures were taken to alleviate distress. Blood samples were promptly harvested from the mouse eyeballs, and the serum was separated by high-speed centrifugation for further analysis. The partial hearts and aortas were preserved in formaldehyde, whereas the others were stored at −80°C for future experiments. Tissue analysis was performed by investigators blinded to group assignments using coded samples.

## Histopathological Staining

Aortic tissues from each group were preserved in 4% paraformaldehyde at low temperature and mounted in OCT compound for sectioning. Sections measuring 8 μm thick were cut using a freezing microtome and fixed in a stationary liquid. These sections were subjected to Oil Red O (ORO) staining following standard protocols to assess atherosclerotic lesion areas in both the entire aorta and aortic root cross sections. Aortic tissues were fixed in neutral formaldehyde for 24 h, processed through an alcohol dehydration series, cleared with xylene, and embedded in paraffin. Paraffin sections (4 μm thick) were prepared and stained with hematoxylin-eosin (HE) after paraffin removal to visualize extracellular lipid components, such as cholesterol crystals and cholesterol esters, along with lesion morphology. To detect vascular collagen deposition, Masson's trichrome staining was performed, according to the manufacturer's instructions. Light microscopy was used to examine pathological changes, and Image-Proplus software (version 6.0) was used to quantify the stained areas. Statistical analysis was performed on the basis of the proportion of positively stained intimal areas relative to the total intimal area.

## Immunohistochemistry Staining

The levels and distribution of the AS marker proteins CD68 and α-smooth muscle actin (α-SMA) in the aortic tissues of each group were evaluated using immunohistochemical techniques. Paraffin-embedded sections were washed with PBS, followed by the application of $H_2O_2$ to block endogenous peroxidase activity. Subsequently, antigen retrieval was performed using citrate buffer solution (pH 6.0). Subsequently, 3% bovine serum albumin solution was applied to block non-specific binding. Specific primary antibodies against CD68 (diluted 1:500) and α-SMA (diluted 1:3000) were added to the sections and incubated overnight. The excess primary antibody was removed by washing, after which a secondary antibody diluent was added and incubated. Color development was achieved using DAB chromogen solution and nuclei were counterstained with hematoxylin. The sections were subsequently dehydrated, cleared, and mounted on

coverslips using a neutral mounting medium. Immunohistochemical results were captured using an optical microscope, and positive staining intensity was quantified using Image-Pro Plus 6.0.

## Measurement of Serum Level of Blood Lipid

Serum was extracted from the blood samples obtained through surgical removal of the eyeballs. Quantification of total cholesterol (TC), high-density lipoprotein cholesterol (HDL-C), low-density lipoprotein cholesterol (LDL-C), and triglycerides (TG) in the serum was conducted using an automated biochemical analyzer (COBAS8000, Roche, Switzerland).

## Measurement of Iron Content Levels

The cut aortic tissue was centrifuged at 4°C and 12000r/min for 10 min to prepare the suspension, and the serum was directly detected after centrifugation under the same conditions. A standard hole and sample hole were set. 5μL iron reducing agent was added to each well and the plate was incubated. Then 100μL iron probe reagent was added, and the mixture was incubated away from light. Finally, the absorbance was measured using an enzymoleter, and the total iron content in the serum and aorta of the mice was calculated according to the manufacturer's instructions.

## Prussian Blue Staining

The aorta tissue sections were subjected to routine deparaffinization and rehydration. The sections were then stained with Prussian blue, washed with PBS, incubated in DAB solution, rinsed with tap water, and dehydrated using a graded alcohol series. Finally, the sections were mounted with neutral resin and observed under an optical microscope to select images.

## Oxidative Stress Indicator Detection

According to the manufacturer's instruction, the catalytic activity of the antioxidant proteins of malondialdehyde (MDA), reduced GSH, 8-OHdG, 4-hydroxynonenal (4HNE) and ROS within artery lysates were measured with MDA activity assay kit (No. A003-1-1, Nanjing, China), and GSH activity assay kit (No. A061-1-1, Nanjing, China), and 8-OHDG activity assay kit (No. H165, Nanjing, China) and 4HNE Activity Assay Kit (No. H268; Nanjing, China) and an ROS assay kit (No. E004-1-1, Nanjing, China). Prior to conducting the measurements with these assay kits, it was imperative to subject the aortic tissues to pretreatment. Subsequently, the tests were performed in accordance with specific instructions for each reagent.

## Transmission Electron Microscopy (TEM)

Aortic tissues were collected and immediately fixed in a solution containing 2.5% glutaraldehyde. The samples were then treated with 1% osmium tetroxide. The aortic tissues were soaked in a mixture of anhydrous acetone and embedding solutions in different proportions at room temperature and then cured at 60 °C. The tissues were cut into 70 nm thick sheets using an ultrathin microtome and placed in a copper mesh. The samples were stained with uranium acetate and citric acid for staining purposes. Finally, the images were visualized using TEM.

## Immunofluorescence Staining

The colocalization of Nrf2 (Abcam; ab92946), HO-1 (Abcam; ab52947), and F4/80 (Abcam; ab16911) in the aortic sinuses was examined by immunofluorescence (IF) staining. IF staining was performed on cryosections of aortic sinuses. The frozen slices were rewarmed and washed with PBS. The tissues were incubated with 3% BSA blocking solution. Tissue sections were incubated overnight with primary antibodies at 4 °C according to the manufacturer's instructions. Subsequently, the secondary antibody was dropped and sealed after the sections were washed with PBS. The corresponding antibody markers were then super-induced. The nuclei were labeled with DAPI and the sections were subjected to 3 rinses with PBS. Subsequently, aortic root tissues were visualized under a fluorescence microscope (U-RFL-T model, OLYMPUS). The expression areas of Nrf2 and HO-1 were quantitatively analyzed using ImageJ software.

## Western Blot Analysis

Frozen aortic tissues were sectioned into smaller pieces and combined with lysis buffer before homogenization and centrifugation at 12,000 rpm for 10 min at 4 °C to collect the supernatant. For the extraction of nuclear proteins, tissue fragments were mixed with CREA, agitated, and placed in an ice bath, followed by the addition of CREB, agitation, and incubation on ice for an additional minute. The mixture was then centrifuged at 14,000 rpm and 4 °C, and the supernatant was harvested as the nuclear protein fraction. Protein concentration was quantified using a BCA protein assay kit. Proteins were mixed with loading buffer in a 4:1 ratio, boiled, cooled, and stored at −80 °C. Separation and stacking gels were prepared for SDS-PAGE and electrophoresis was performed. The antibody incubation process involved washing the PVDF membrane with 1xTBST, overnight incubation with the primary antibody at 4 °C, washing with TBST, and incubation with the secondary antibody at room temperature. Antibodies catalogue numbers see Supplementary File 1. For blot development, the membrane was washed three times with 1xTBST, immersed in a 1:1 ECL reagent mix, and visualized using the imaging system.

## Real-Time Quantitative Reverse Transcription-Polymerase Chain Reaction (PCR)

Mouse aorta tissues were homogenized in liquid nitrogen and lysed using the TRIzol reagent. Total RNA was isolated via chloroform extraction, followed by isopropanol precipitation, and purification with 75% ethanol. The RNA was then reconstituted in DEPC-treated water and stored at −80°C. The isolated RNA was converted into complementary DNA using a reverse transcription kit, and the complementary DNA was stored at −20°C. The primer sequences used are listed in Table 1. The expression levels of the target genes were quantified using real-time PCR. PCR was performed using a thermal cycling protocol that included an initial pre-denaturation step, followed by 40 cycles of denaturation and annealing/extension. β-actin was used as an internal control to standardize the expression data.

## Statistical Analysis

The data were analyzed using SPSS 26.0. Univariate analysis of variance or independent *t*-tests were used for normally distributed variables with equal variance. When these assumptions were violated, the Mann–Whitney *U*-test was used. Outcomes are reported as mean ± SD. Statistical significance was set at $P < 0.05$, with $P < 0.01$ indicating a highly significant result.

# Results

## PD and HLF Protect Against AS Development in HFD-Induced ApoE$^{-/-}$ Mice

A model of HFD-induced AS was established in ApoE$^{-/-}$ mice, and the effects of PD and HLF on the progression of atherosclerotic lesions in ApoE$^{-/-}$ mice were examined. Throughout the experimental period, no abnormal mortality was recorded in any of the cohorts. ApoE$^{-/-}$ mice subjected to the HFD regimen exhibited no significant variation in body weight compared with the ND group. As the study progressed into the 13th week, the rate of weight accretion in the SVT- and PH-administered mice started to diminish. However, no appreciable distinction was observed between the cohorts (Figure 1A). After the 8-week treatment period, atherosclerotic lesion formation was assessed using en face ORO

**Table 1** Primer Sequences

| Primer | Forward | Reverse |
|---|---|---|
| NRF2 | ACTCAAATCCCACCTTAAACAC | GTCACAGCCTTCAATAGTCCC |
| HO-1 | CGCAACAAGCAGAACCCAG | CCAGTGAGGCCCATACCAG |
| GPX4 | TACTGCAACAGCTCCGAGTTCCT | GTGACGATGCACACGAAACCCC |
| TFR1 | GCGAGATGAACACTATGTGA | CACTGGGTCTAAGTTACCAT |
| SLC7A11 | ATTCTCATTAGCAGTCCCGAT | AGATGCGACGTAGAATAACCT |
| FPN1 | AGAATCGGTCTTTGGTCCTT | TGCACACCATTGATAATGCCTC |
| FTH1 | AAACCAGACCGTGATGACT | GGATCATTCTTGTCAGTAGCCAG |
| β-actin | CTCCTGAGCGCAAGTACTCT | TACTCCTGCTTGCTGATCCAC |


https://doi.org/10.2147/JIR.S530995

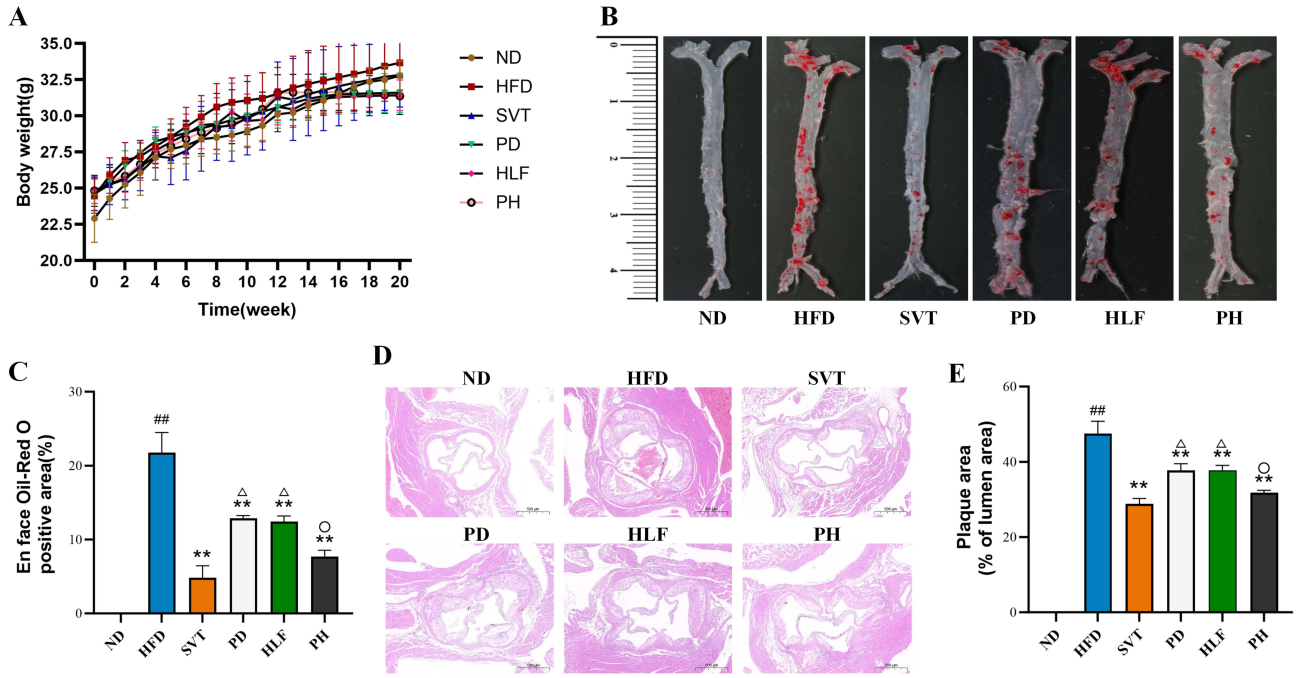


**Figure 1** Treatment with PD and HLF can effectively inhibit the progression of AS in ApoE$^{-/-}$ mice. (**A**) Showed the body weight of mice in each group; (**B**) Displayed representative images of ORO staining of the aorta; (**C**) Presented quantitative analysis of ORO staining of the aorta; (**D**) Displayed representative images of HE staining of the aorta at 40× magnification; (**E**) Presented quantitative analysis of HE staining of the aorta.
**Notes**: $^{\#\#}P<0.01$ vs ND group; $^{**}P<0.01$, vs HFD group; $^{\Delta}P<0.05$, vs PH group; $^{\circ}P>0.05$ vs SVT group.

staining. Visually, the aorta of the ND group appeared smooth and unobstructed, whereas that of the HFD group exhibited the most extensive plaque formation at the aortic arch and root. All treatment groups displayed a reduction in plaque burden compared with the HFD group, albeit to varying degrees (Figure 1B and C). Histological examination of aortic root sections via HE staining further revealed a marked and progressive decrease in the size of the necrotic core in drug-treated mice (Figure 1D and E).

## PD and HLF Promote Plaque Stability in HFD-Induced ApoE$^{-/-}$ Mice

The plaque vulnerability index is a critical indicator of AS progression. ORO staining of aortic root sections showed pronounced lipid accumulation within the plaques in the HFD group. The administration of PD and HLF markedly reduced lipid accumulation (Figure 2A and B). Masson's staining was used to quantify the collagen content within the plaques. Consistent with our hypothesis, treatment with PD and HLF resulted in a significant increase in collagen content within plaques (Figure 2C and D). Furthermore, the expression of macrophage marker (CD68) and smooth muscle cell marker (α-SMA) was investigated via immunohistochemical (IHC) analysis of atherosclerotic plaques. In the plaques of ApoE$^{-/-}$ mice, PD and HLF treatment suppressed the expression of CD68 (Figure 2E and F) and enhanced the expression of α-SMA (Figure 2G and H). These data suggest that PD and HLF, particularly in conjunction, can diminish extracellular lipid deposition and increase collagen fiber content, thereby substantially decreasing the plaque vulnerability index (Figure 2I) and improving atherosclerotic plaque stability.

## PD and HLF Regulated the Blood Lipid in ApoE$^{-/-}$ Mice

The progression of atherosclerotic plaques has been previously reported to be correlated with dysfunction in lipid metabolism. Consequently, we measured blood lipid levels (Figure 3A–D). The HFD group exhibited a marked elevation in TG, TC, and LDL-C levels, coupled with a reduction in HDL-C levels, compared to the ND group. In contrast to the HFD group, the various treatment groups showed significantly decreased TC, TG, and LDL-C levels, along with a significant improvement in HDL-C levels. No discernible differences in the serum HDL and TG levels were observed between the PH and SVT groups. Collectively, these findings suggest that both PD and HLF mitigated AS development and ameliorated the lipid profile of ApoE$^{-/-}$ mice.

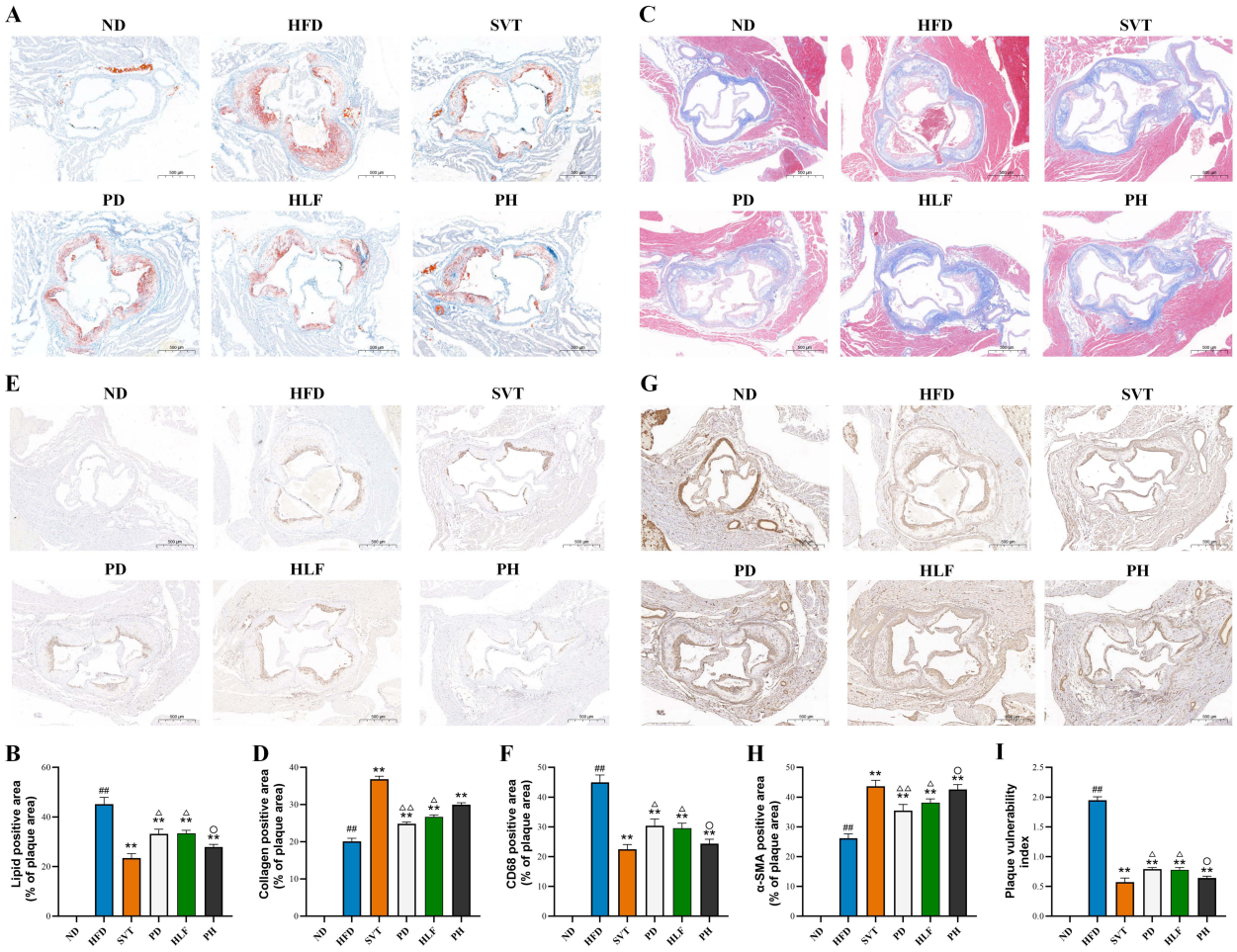


**Figure 2** Treatment with PD and HLF can effectively inhibit plaque development in ApoE$^{-/-}$ mice. (**A**) Showed representative frozen section images of the aortic arch stained with ORO; (**B**) Displayed the quantitative analysis of ORO staining; (**C**) Presented representative paraffin section images of the aortic root stained with Masson's trichrome for necrotic cores; (**D**) Displayed the quantitative analysis of Masson staining; (**E**) Presented representative IHC stained images with CD68 antibody; (**F**) Displayed the quantitative analysis of CD68 staining; (**G**) Presented representative IHC stained images with α-SMA antibody; (**H**) Displayed the quantitative analysis of α-SMA staining; (**I**) Represented the plaque vulnerability index. All images were shown at 40× magnification. (**I**) Represented the plaque vulnerability index.
**Notes**: $^{\#\#}P<0.01$ vs ND group; $^{**}P<0.01$, vs HFD group; $^{\Delta}P<0.05$, $^{\Delta\Delta}P<0.01$ vs PH group; $^{\circ}P>0.05$ vs SVT group.

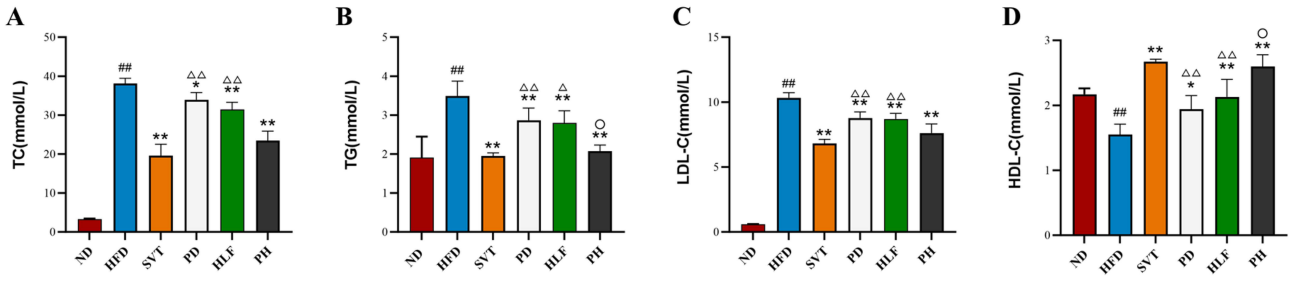


**Figure 3** Treatment with PD and HLF can regulate lipid metabolism in ApoE$^{-/-}$ mice. (**A–D**) Serum TC, TG, LDL-C and HDL-C were shown successively.
**Notes**: $^{\#\#}P<0.01$ vs ND group; $^{*}P<0.05$, $^{**}P<0.01$, vs HFD group; $^{\Delta}P<0.05$, $^{\Delta\Delta}P<0.01$ vs PH group; $^{\circ}P>0.05$ vs SVT group.

## PD and HLF Decreased Level of Iron in Atherosclerotic Plaques

Ferroptosis is characterized by disrupted iron metabolism. Quantitative analysis of iron in the aorta and serum revealed significantly higher ferrous iron levels in the HFD group than in the ND group (Figure 4A and B). Treatment with PD or HLF reversed the HFD-induced iron accumulation. Prussian blue staining confirmed reduced aortic iron deposition


https://doi.org/10.2147/JIR.S530995

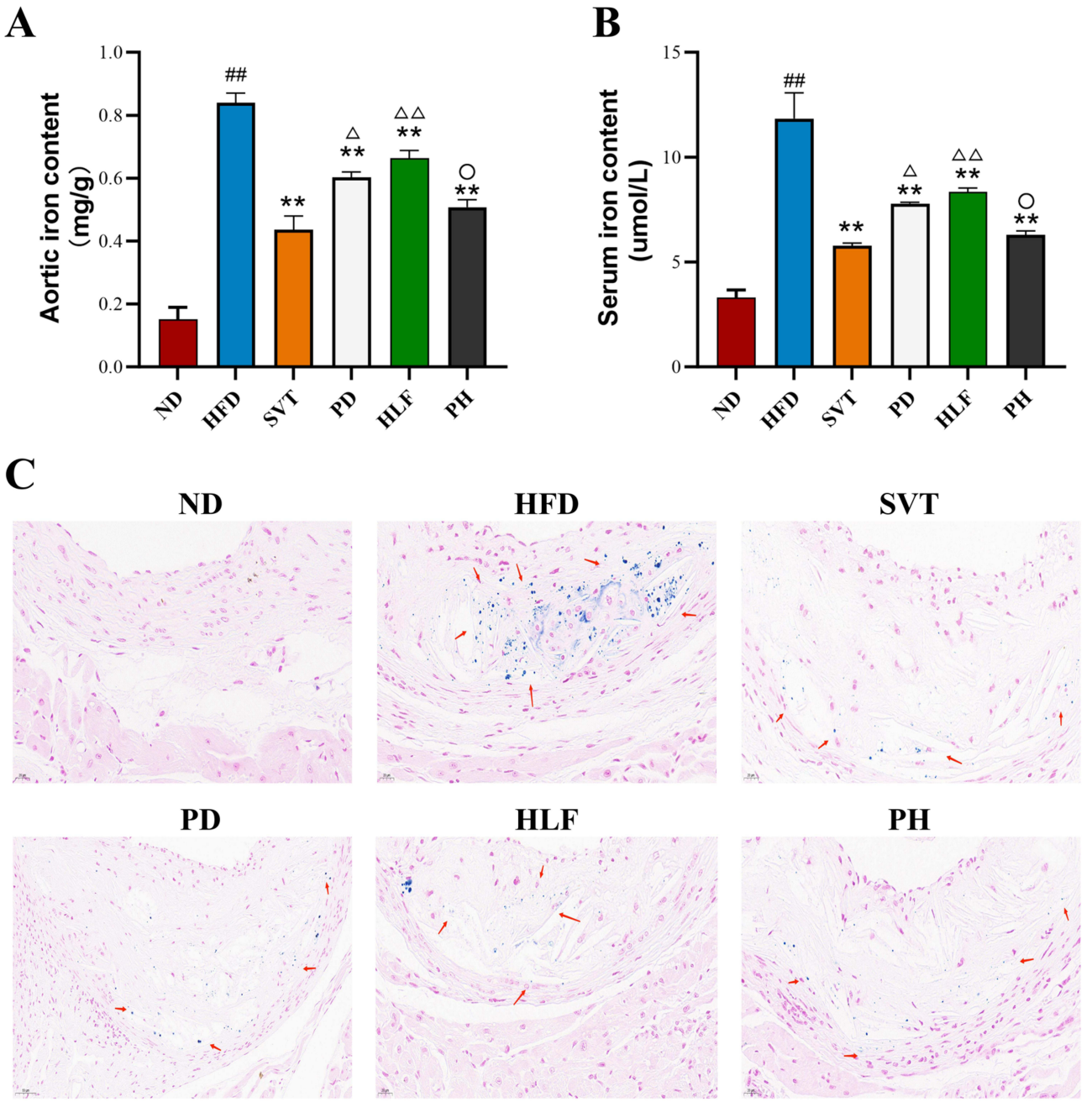


**Figure 4** Treatment with PD and HLF could regulate iron levels in ApoE$^{-/-}$ mice. (**A** and **B**) Showed the ferric iron content in aortic tissue and serum ferric iron content, respectively. (**C**) Presented the results of Prussian blue staining of the aorta at 40× magnification (red arrows indicate evident increase in iron aggregates).
**Notes**: $^{\#\#}P<0.01$ vs ND group; $^{**}P<0.01$, vs HFD group; $^{\triangle}P<0.05$, $^{\triangle\triangle}P<0.01$ vs PH group; $^{\circ}P>0.05$ vs SVT group.

following PD and HLF intervention (Figure 4C), suggesting their potential to mitigate ferroptosis by regulating iron homeostasis in AS patients. The findings of this study indicate that the inhibitory effects of PD and HLF on iron overload may be one of the mechanisms by which these compounds ameliorate AS. Notably, the combined use of PD and HLF demonstrated an efficacy comparable to that of SVT.

## PD and HLF Improved Lipid Peroxidation in Atherosclerotic Plaques

Given that excessive lipid peroxidation is a direct driver of ferroptosis, we measured key indicators of lipid peroxidation in the aorta, including ROS, MDA, GSH, 8-OHdG, and 4-HNE (Figure 5A–E). Compared to the ND group, the HFD

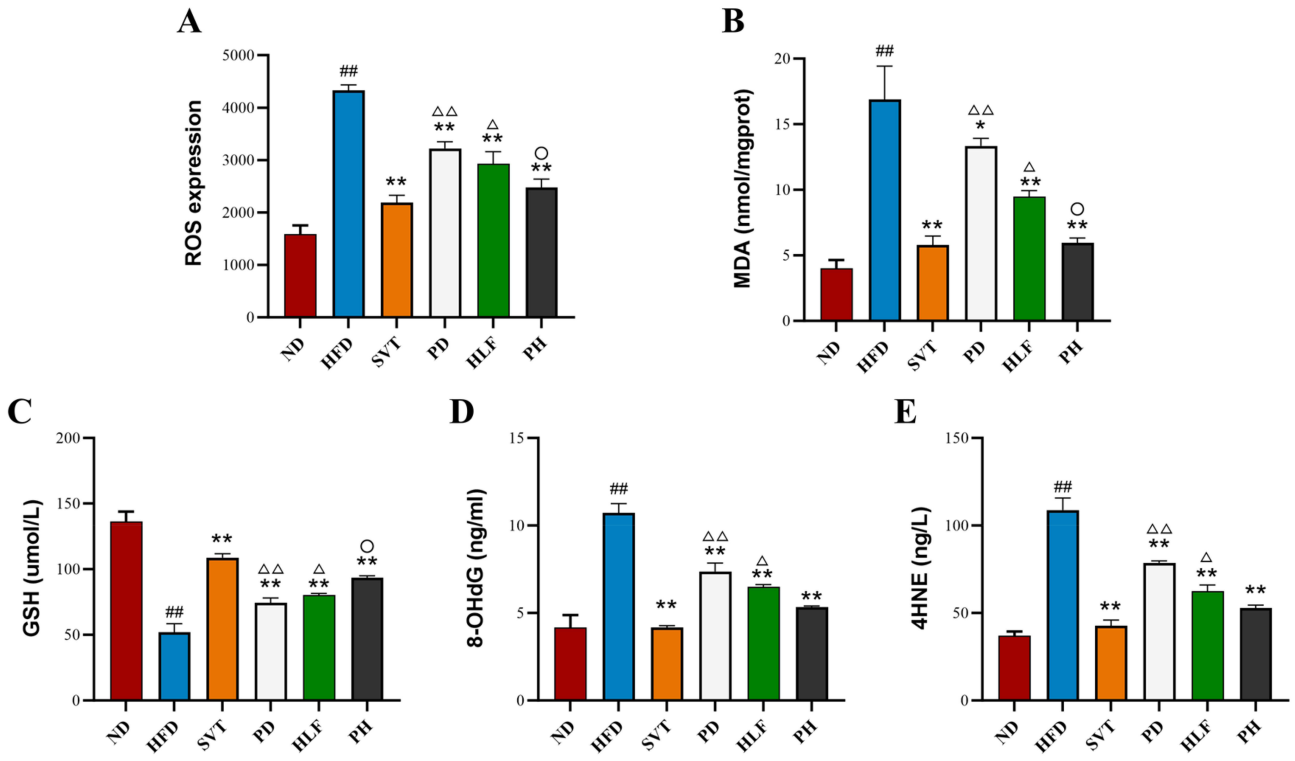


**Figure 5** Treatment with PD and HLF can modulate lipid peroxidation levels in ApoE$^{-/-}$ mice. (**A**–**E**) Showed the levels of ROS, MDA, GSH, 8-OHdG, and 4HNE in aortic tissue, respectively.

**Notes**: $^{\#\#}P<0.01$ vs ND group; $^{*}P<0.05$, $^{**}P<0.01$, vs HFD group; $^{\triangle}P<0.05$, $^{\triangle\triangle}P<0.01$ vs PH group; $^{\circ}P>0.05$ vs SVT group.

group exhibited significantly elevated levels of ROS, MDA, 4-HNE, and 8-OHdG, along with a substantial decrease in GSH levels. In contrast, all treatment groups showed significantly reduced levels of ROS, MDA, 4-HNE, and 8-OHdG, and a remarkable increase in GSH compared to the HFD group.

## PD and HLF Improved Mitochondrial Morphology

TEM was used to assess macrophage mitochondrial morphology within the aortic plaques (Figure 6). Mitochondria from the ND group appeared healthy with oval shapes, intact membranes, and well-structured cristae. In the HFD group, mitochondria displayed characteristic signs of ferroptosis, such as swelling, loss of cristae, and elevated membrane density. The SVT treatment group exhibited an increase in mitochondrial count and a decrease in swelling and ferroptotic damage compared to the HFD group. Significantly, the PD, HLF, and PH treatment groups showed a reduction in swollen mitochondria and ferroptotic features compared with the HFD group.

## PD and HLF Inhibited Ferroptosis Mediated by the Nrf2 Nuclear Translocation in ApoE$^{-/-}$ Mice

Nuclear translocation of Nrf2 in macrophages triggers ferroptosis, which plays a fundamental role in the progression of AS. We also performed IF staining of the key proteins Nrf2 (Figure 7A and B) and HO-1 (Figure 7C and D) in the Nrf2/HO-1/GPX4 axis. The results demonstrated that relative to the ND group, the plaques in the HFD group were enriched with a large number of F4/80-labeled macrophages, and the co-localization of F4/80 with Nrf2 and HO-1 was increased, indicating a mild abnormal activation of Nrf2 within macrophages. Compared with the HFD group, the co-localization in the plaques of each treatment group was significantly enhanced, and the degree of Nrf2 nuclear translocation was higher. Among these, colocalization enhancement was more pronounced in the PH group, with no statistically significant difference compared to the SVT group.


https://doi.org/10.2147/JIR.S530995

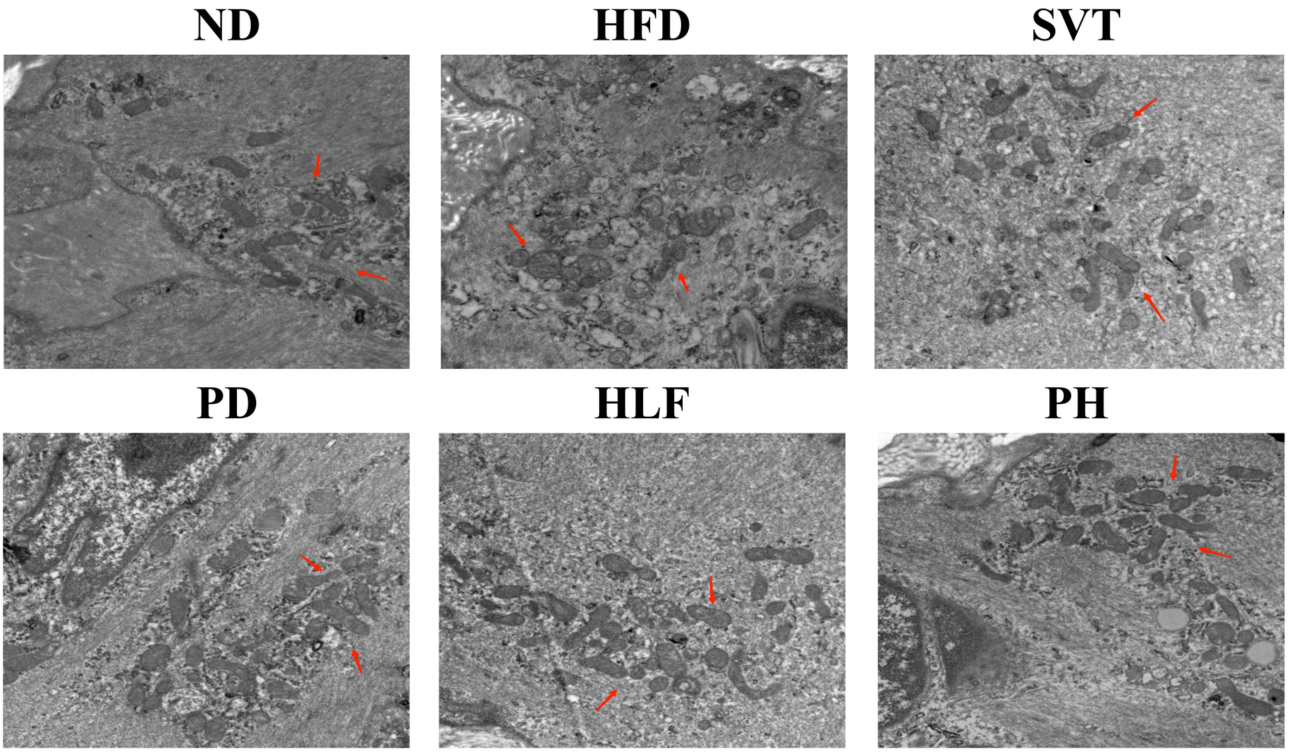


**Figure 6** Treatment with PD and HLF could improve mitochondrial morphology in ApoE-/- mice. This figure showed the morphology of macrophages in aortic plaques observed by TEM at 20000× magnification (red arrows indicate typical mitochondrial morphology of the group).

## PD and HLF Activate the Expression of Nrf2/HO-1/GPX4 Axis Related to Ferroptosis

The Nrf2/HO-1/GPX4 axis is a well-established pathway mediating ferroptosis. Therefore, we examined the mRNA expression in ApoE$^{-/-}$ mice (Figure 8A–G). PCR results indicated that, compared to the ND group, the expression of Nrf2, HO-1, and TFR1 mRNA increased in the HFD group, while the mRNA expression of GPX4, SLC7A11, FPN1, and FTH1 was considerably downregulated. All treatment groups showed consistent and statistically significant effects; they increased the mRNA expression of Nrf2, HO-1, GPX4, SLC7A11, FPN1, and FTH1 while simultaneously reducing TFR1 mRNA levels. Among these, the improvement was most notable in the PH group, and there was no statistically significant difference compared to the SVT group.

## PD and HLF Inhibited Ferroptosis via Nrf2/HO-1/GPX4 Axis

To elucidate the mechanisms underlying the anti-atherosclerotic effects of PD and HLF, Western blotting was used to measure the expression levels of the Nrf2/HO-1/GPX4 axis (Figure 9A–I). The results demonstrated that the expression of nuclear Nrf2, HO-1, and TFR1 proteins increased in the HFD group, whereas the expression of cytoplasmic Nrf2, GPX4, SLC7A11, FPN1, and FTH1 proteins was significantly downregulated. Following treatment with PD and HLF, the expression of nuclear Nrf2, HO-1, GPX4, SLC7A11, FPN1, and FTH1 increased, whereas the expression of cytoplasmic Nrf2 and TFR1 decreased. However, no significant differences in the expression levels of these proteins were observed between the PH and SVT groups.

# Discussion

Atherosclerotic plaque instability is a major cause of CVD, and is associated with elevated mortality rates and critical cardiac incidents.[29] Currently, a growing body of evidence demonstrates that natural compounds play a pivotal role in the prevention and treatment of AS.[23,25] Classically, it been theorized that AS is characterized by “Blood Stasis” and “Blood Heat”, which is a major pathogenesis of ASCVD. Our previous research confirmed that Polygonum cuspidatum and hawthorn can improve inflammation and clinical symptoms in patients with unstable angina. PD and HLF are bioactive

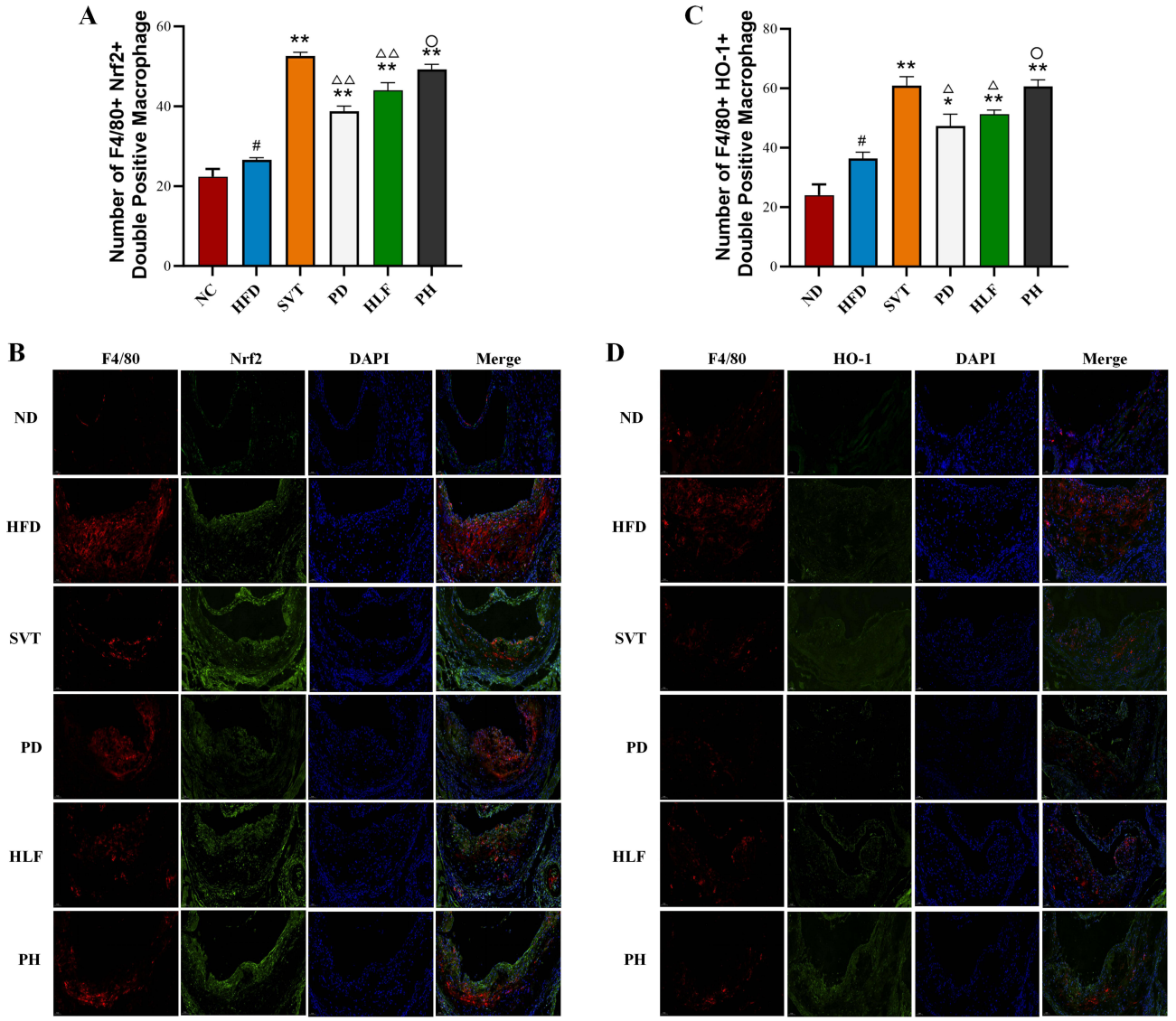


**Figure 7** Treatment with PD and HLF could inhibit ferroptosis in ApoE$^{-/-}$ mice via Nrf2 nuclear translocation. (**A**) Provided the quantitative analysis results of the IF staining for Nrf2; (**B**) Presented IF staining for Nrf2; (**C**) Provided the quantitative analysis results of the IF staining for HO-1; (**D**) Presented IF staining for HO-1.
**Notes**: $^{\#}P<0.05$ vs ND group; $^{*}P<0.05$, $^{**}P<0.01$, vs HFD group; $^{\triangle}P<0.05$, $^{\triangle\triangle}P<0.01$ vs PH group; $^{\circ}P>0.05$ vs SVT group.

constituents derived from Polygonum cuspidatum and Hawthorn, respectively, and have been patented and approved as TCM drugs for the prevention and treatment of AS. Our basic research has already proven that PD or HLF used alone can reduce plaque formation.[23,25,26] Ferroptosis, an emerging type of programmed cell death, has been identified as a potential therapeutic target for AS.[14] However, the specific mechanism by which the PH combination exerts its effects in the treatment of AS remains to be elucidated. We employed ApoE$^{-/-}$ mice to comprehensively investigate the mechanistic role of PH combination in enhancing atherosclerotic plaque stability and its potential effects on ferroptosis.

Lipid accumulation in the arterial wall is a key event in the formation of atherosclerotic lesions. In this study, we first assessed whether PH combination treatment affects body weight and serum lipid content. The results showed that the body weight and serum levels of TC, TG, and LDL-C in the HFD group were significantly higher than those in the ND group. Notably, PH combination led to a significant reduction in body weight and serum levels of LDL-C, TC, and TG. The effects of PH combination were better than those of PD or HLF alone. The key pathological hallmarks of unstable plaques are decreased collagen content and fiber cap thickness. Furthermore, we examined the potential therapeutic effects of the PH combination on pathological damage to aortic morphology. In our study, PH combination treatment


https://doi.org/10.2147/JIR.S530995

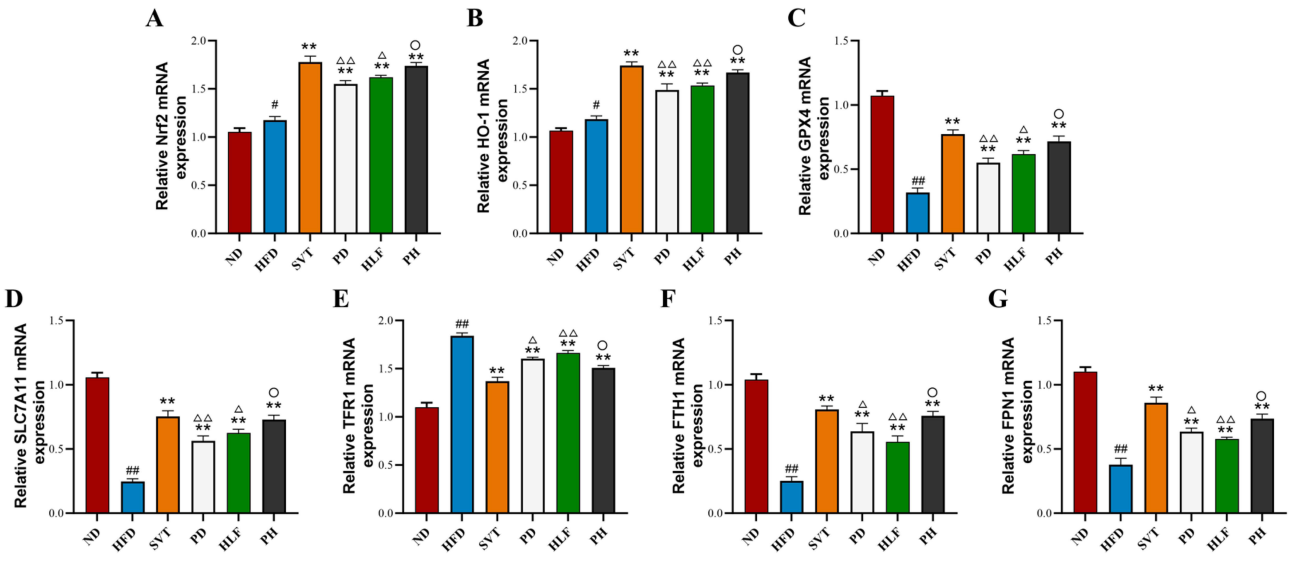


**Figure 8** Treatment with PD and HLF could modulate the mRNA expression of the Nrf2/HO-1/GPX4 axis in ApoE$^{-/-}$ mice. (**A**–**G**) Showed the relative mRNA expression of Nrf2, HO-1, GPX4, SLC7A11, TFR1, FTH1, and FPN1 in the aorta, respectively.
**Notes**: $^{\#}P<0.05$, $^{\#\#}P<0.01$ vs ND group; $^{**}P<0.01$, vs HFD group; $^{\triangle}P<0.05$, $^{\triangle\triangle}P<0.01$ vs PH group; $^{\circ}P>0.05$ vs SVT group.

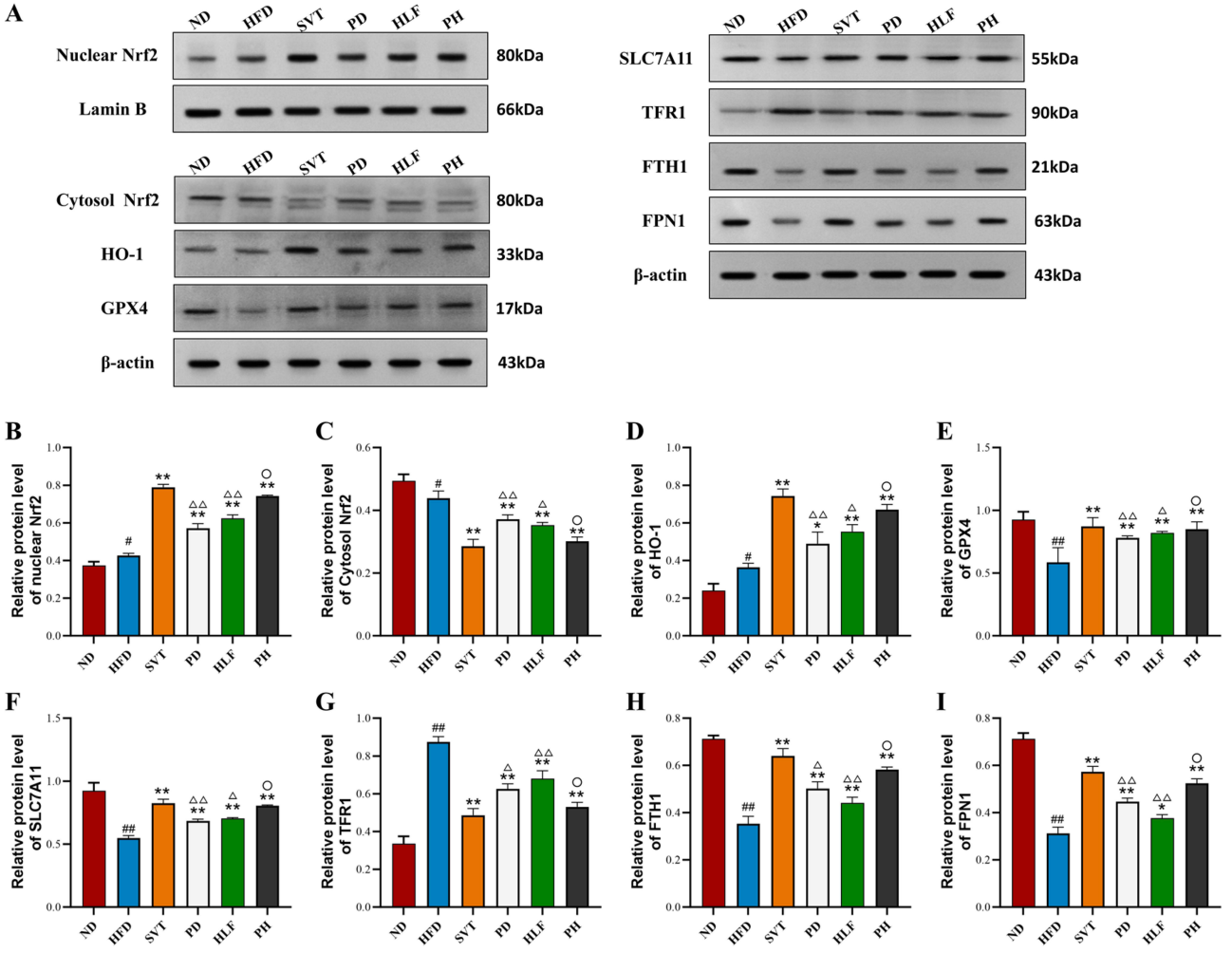


**Figure 9** Treatment with PD and HLF could modulate the protein expression of the Nrf2/HO-1/GPX4 axis in ApoE$^{-/-}$ mice. (**A**) Showed representative Western blot bands. (**B**–**I**) Showed the relative protein expression of nuclear Nrf2, cytosolic Nrf2, HO-1, GPX4, SLC7A11, TFR1, FTH1, and FPN1 in the aorta, respectively.
**Notes**: $^{\#}P<0.05$, $^{\#\#}P<0.01$ vs ND group; $^{*}P<0.05$, $^{**}P<0.01$, vs HFD group; $^{\triangle}P<0.05$, $^{\triangle\triangle}P<0.01$ vs PH group; $^{\circ}P>0.05$ vs SVT group.

reduced plaque area and lipid deposition, and increased collagen content, suggesting that PH combination promotes more stable plaques. We employed IHC techniques to specifically label macrophages and smooth muscle cells and observed changes in the expression of CD68 and α-SMA in the artery tissues of different treatment groups. The results obtained from IHC staining indicated that the PH group had an increased distribution of α-SMA and reduced distribution of CD68 in ApoE$^{-/-}$ mice, indicating the possibility that PH combination intervention could reduce plaque vulnerability. Taken together, these experimental findings suggest that PH combination treatment significantly reduced plaque deposition size and lipid area, increased collagen content, and thickened fibrous cap compared to the HFD group or single drug treatment. Thus, these results indicate that the combination of PD and HLF significantly enhanced atherosclerotic plaque stability and alleviated AS severity.

Ferroptosis, a recently discovered form of programmed cell death, is closely associated with the pathological processes of AS.[14] Several studies have confirmed that ferroptosis is characterized by iron accumulation and lipid peroxidation, and the inhibition of ferroptosis may be a promising therapeutic strategy for AS therapy.[14,30] AS lesions are frequently accompanied by imbalance in iron homeostasis. Excessive intracellular iron impairs antioxidant mechanisms via the Fenton reaction, which ultimately exacerbates necrotic core formation and plaque instability. Morphologically, ferroptotic cells exhibit shrunken mitochondria with reduced or no mitochondrial ridges. Accordingly, TEM was used to examine the ultrastructure of the mitochondria in aortic tissue. TEM results showed that the PH group manifested reduced mitochondrial volume and rupture or disappearance of the mitochondrial crista. Subsequently, Prussian blue staining was used to observe the aggregation of iron ions in aortic tissue. Our results indicate that the PH combination reduced the aggregation of iron ions in the aorta. Owing to the vital role of iron overload in ferroptosis, we assessed iron content in the serum and aortic tissues. Quantitative analysis of iron content showed that, compared with the ND group, the HFD group showed increased expression of iron in both the aortic tissue and serum. Treatment with PH significantly suppressed iron accumulation in the serum and aortic tissue of ApoE$^{-/-}$ mice compared to that in the HFD group or single drug treatment. Accumulated evidence suggested that excessive lipid peroxidation is considered an independent risk factor of AS and the main drivers of ferroptosis.[14,31] ROS, MDA, 4-HNE, GSH, and 8-OHdG are key proteins related to lipid peroxidation that can be activated through oxidative stress pathways, and their expression directly reflects the extent of lipid peroxidation. In this study, HFD increased ROS, MDA, 4-HNE, and 8-OHdG generation, and decreased GSH levels in ApoE$^{-/-}$ mice. The PH combination significantly reduced ROS, MDA, 4-HNE, and 8-OHdG generation and increased GSH levels compared with PD or HLF alone. In summary, these results indicate that PH combination significantly decreased iron content and oxidative damage in ApoE$^{-/-}$ mice.

To further investigate the specific molecular mechanism by which PH combination inhibits ferroptosis in AS, we examined the role of the Nrf2/HO-1/GPX4 axis. Extensive research has clarified the effective role of Nrf2/HO-1/GPX4 axis activation in regulating ferroptosis.[20,32] Nrf2 is involved in the production of antioxidative genes that protect cells from oxidative damage resulting from injury and inflammatory processes.[16] As downstream transcriptional target of Nrf2, HO-1 plays a pivotal role in the regulation of oxidative stress.[33] Previous animal studies reported that activation of Nrf2 can effectively retard atherosclerotic progression in athero-prone mice.[18,34] To further clarify the molecular mechanism by which PH combination inhibits ferroptosis in AS, we performed IF assays to examine the location of Nrf2, HO-1, and F4/80. Our IF analysis revealed that Nrf2 translocates from the cytoplasm to the nucleus during AS, thereby activating transcription of the downstream target gene HO-1 to limit ferroptosis. At present, it is believed that lipid peroxidation in ferroptosis is mainly caused by system Xc$^-$ and GPX4.[35] GPX4 is an important antioxidant enzyme that regulates Nrf2 and can inhibit ferroptosis by diminishing lipid peroxides.[36] SLC7A11 is the main structural component of the Xc cell system$^-$ and plays a vital role in maintaining redox homeostasis.[9] The results of Western blot analysis confirmed that compared with the HFD group, PH combination significantly promoted Nrf2 nuclear translocation and increased the expression of HO-1, GPX4, and SLC7A11 in aortic tissue. Another characteristic of ferroptosis is the excessive accumulation of iron, which may be due to dysfunction of iron-regulatory proteins.[37] Notably, previous studies have verified that changing Nrf2 expression in the nucleus can influence downstream iron-related proteins, such as TFR1, FTH1, and FPN1, resulting in increased iron efflux and decreased intracellular iron content.[38] FPN1 and TFR1 play central roles in mediating cellular iron uptake and export, whereas FTH1 is involved in intracellular iron storage.[39] Therefore, we determined the expression levels of the iron metabolism marker genes. Our findings

demonstrate that either PD or HLF alone can upregulate Nrf2 levels, activate the SLC7A11/GSH/GPX4 antioxidant axis, and thereby reduce lipid peroxidation toxicity. Concomitantly, both compounds mitigate iron overload and attenuate the Fenton reaction via upregulation of FTH1 and HO-1 expression, thereby inhibiting ferroptosis. Notably, similar regulatory effects on ferroptotic pathways have been documented for other botanical extracts (eg, Astragaloside IV,[40] Silibinin,[41] Baicalein[42]) in models of distinct pathologies. Furthermore, in ApoE$^{-/-}$ mice, PH combination significantly increased the expression levels of FPN1 and FTH1 while decreasing TFR1 expression compared to both the HFD group and the groups receiving either drug alone. The relevant pathways are shown in Figure 10. Collectively, our experimental results demonstrate that the PH combination stabilizes plaques by enhancing iron transport/storage function and boosting antioxidant capacity through the synergistic action of PD and HLF. Notably, the therapeutic efficacy of PH over monotherapy stems from potentiated synergistic effects, which have been similarly documented in other studies.[43]

This study demonstrates that the PH combination stabilizes atherosclerotic plaques by modulating ferroptosis via the Nrf2/HO-1/GPX4 axis. However, certain limitations should be acknowledged. First, the lack of a PH combined with ferroptosis inhibitor group (eg, ferrostatin-1) impedes comprehensive mechanistic validation of ferroptosis as the primary pathway. Second, comparisons with other plant-derived anti-atherosclerotic agents (eg, resveratrol or berberine) were not performed, limiting the evaluation of PH's relative efficacy among botanical therapeutics. Third, translational applications require further investigation, as findings derived from ApoE$^{-/-}$ mice necessitate validation in larger animal models and human studies to assess pharmacokinetics, safety profiles, and clinical outcomes. Additionally, dose-response relationships for PH and potential synergistic mechanisms beyond the Nrf2 axis remain uncharacterized. Addressing these aspects will enhance the therapeutic rationale for PH in atherosclerotic plaque management, strengthening its viability as an alternative to statin therapy.

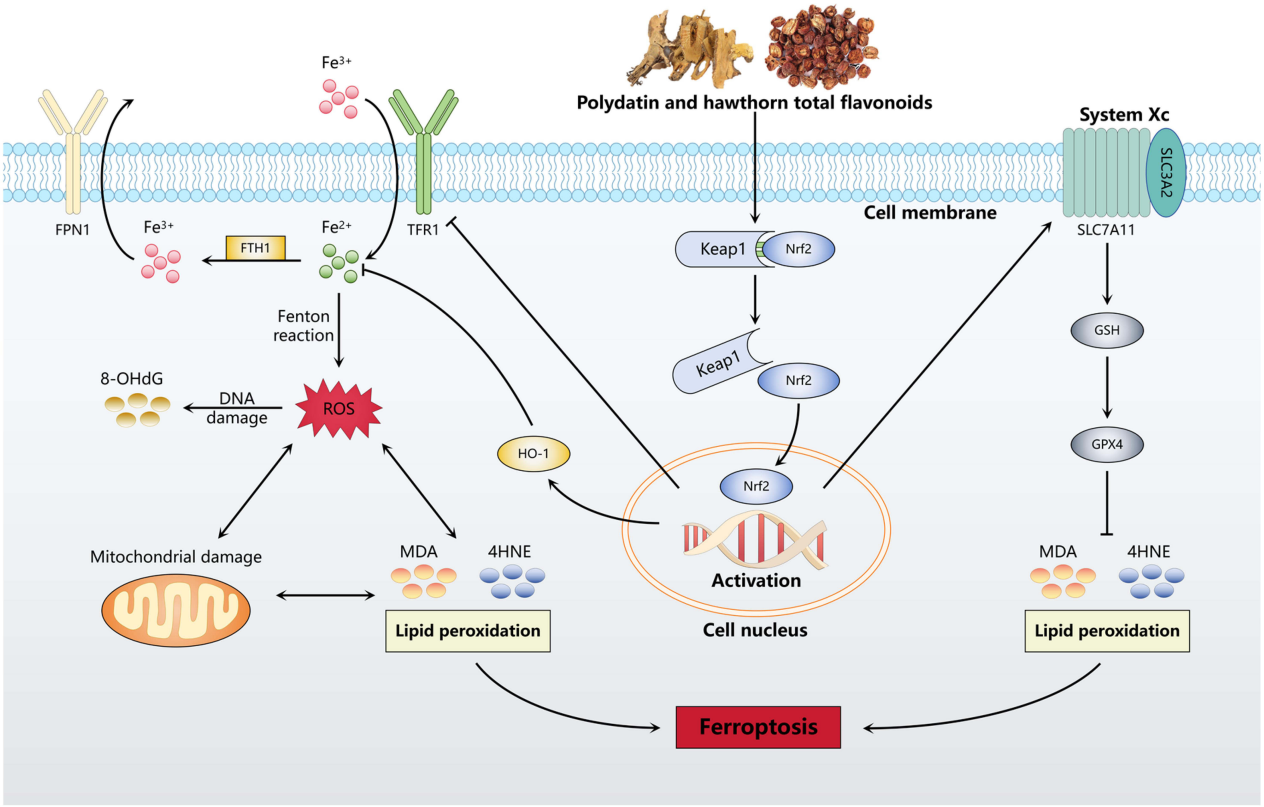


**Figure 10** Schematic representation of the mechanism by which the PH combination inhibits ferroptosis. The PH combination activates the Nrf2 signaling pathway by promoting the dissociation of Nrf2 from Keap1. Activated Nrf2 translocates to the nucleus and upregulates the expression of HO-1, GPX4 and SLC7A11, which could reduce lipid peroxidation and oxidative stress, thereby inhibiting ferroptosis. Additionally, the PH combination regulates iron metabolism by modulating the expression of FPN1, FPN1 and TFR1, which could reduce iron overload. The reduction in lipid peroxidation and iron overload ultimately leads to the stabilization of vulnerable plaques.

## Conclusion

In summary, our study demonstrated that the PH combination is superior to both PD and HLF used individually to stabilize vulnerable plaques. PH combination enhances plaque stability by ameliorating iron metabolism disorders and lipid peroxidation in ApoE$^{-/-}$ mice. Mechanistically, this effect is associated with activation of the Nrf2/HO-1/GPX4 axis. Collectively, these findings provide a potential molecular basis for clinical inhibition of vulnerable atherosclerotic plaques.

## Abbreviations

α-SMA, α-smooth muscle actin; FTH1, ferritin heavy chain 1; FPN1, ferroportin 1; GSH, glutathione; GPX4, glutathione peroxidase 4; HDL-C, high-density lipoprotein cholesterol; HFD, high-fat diet; HE, hematoxylin-eosin; HLF, hawthorn leave flavonoids; HO-1, heme oxygenase-1; IF, immunofluorescence; LDL-C, low-density lipoprotein cholesterol; MDA, malondialdehyde; mTOR, mammalian target of rapamycin; ND, normal diet; Nrf2, nuclear factor erythroid 2-related factor 2; NLRP3, Nucleotide oligomerization (NOD)-like receptor (NLR) family pyrin domain-containing protein 3; ORO, Oil-Red-O; ox-LDL, oxidized low-density lipoprotein; PD, polydatin; PH, polydatin and hawthorn leave flavonoids; SVT, simvastatin; TC, total cholesterol; TEM, transmission electron microscopy; TFR1, transferrin receptor protein 1; TG, triglyceride; SLC7A11, solute carrier family 7 member 11; 4HNE, 4-hydroxynonenal; 8-OHdG, 8-hydroxy-2 deoxyguanosine.

## Data Sharing Statement

The datasets used and/or analyzed during the current study are available from the corresponding author upon reasonable request.

## Ethics Approval and Consent to Participate

The study was conducted in compliance with both the ARRIVE guideline 2.0 and the Chinese guidelines for welfare and ethics for laboratory animals, as approved by the Animal Ethics Committee of Xiyuan Hospital, China Academy of Chinese Medical Sciences (Approval No. 2021XLC020-3).

## Consent for Publication

The author gives consent for the publication of identifiable details, which can include the data and content to be published in the above Journal and Article.

## Funding

The Beijing Natural Science Foundation (No. 7242257), Capital's Funds for Health Improvement and Research (No. 2022-2-4172), and Hospital Capability Enhancement Project of Xiyuan Hospital, CACMS (XYZX0201-09).

## Disclosure

The authors declare that they have no competing interests in this work.

## References

1. Hetherington I, Totary-Jain H. Anti-atherosclerotic therapies: milestones, challenges, and emerging innovations. *Mol Ther*. 2022;30(10):3106–3117. doi:10.1016/j.ymthe.2022.08.024
2. Bentzon JF, Otsuka F, Virmani R, et al. Mechanisms of plaque formation and rupture. *Circ Res*. 2014;114(12):1852–1866. doi:10.1161/circresaha.114.302721
3. Hwang IC, Kim CH, Kim JY, et al. Rate of change in 10-year atherosclerotic cardiovascular disease risk and its implications for primary prevention. *Hypertension*. 2023;80(8):1697–1706. doi:10.1161/hypertensionaha.122.20678
4. Morrison AM, Sullivan AE, Aday AW. Atherosclerotic disease: pathogenesis and approaches to management. *Med Clin North Am*. 2023;107(5):793–805. doi:10.1016/j.mcna.2023.04.004
5. Ueki Y, Itagaki T, Kuwahara K. Lipid-lowering therapy and coronary plaque regression. *J Atheroscler Thromb*. 2024;31(11):1479–1495. doi:10.5551/jat.RV22024
6. De Meyer GRY, Zurek M, Puylaert P, et al. Programmed death of macrophages in atherosclerosis: mechanisms and therapeutic targets. *Nat Rev Cardiol*. 2024;21(5):312–325. doi:10.1038/s41569-023-00957-0
7. Lin X, Ouyang S, Zhi C, et al. Focus on ferroptosis, pyroptosis, apoptosis and autophagy of vascular endothelial cells to the strategic targets for the treatment of atherosclerosis. *Arch Biochem Biophys*. 2022;715:109098. doi:10.1016/j.abb.2021.109098

8. Yang S, Li Y, Zhou L, et al. Copper homeostasis and cuproptosis in atherosclerosis: metabolism, mechanisms and potential therapeutic strategies. *Cell Death Discov*. 2024;10(1):25. doi:10.1038/s41420-023-01796-1
9. Dixon SJ, Lemberg KM, Lamprecht MR, et al. Ferroptosis: an iron-dependent form of nonapoptotic cell death. *Cell*. 2012;149(5):1060–1072. doi:10.1016/j.cell.2012.03.042
10. Ni D, Lei C, Liu M, et al. Cell death in atherosclerosis. *Cell Cycle*. 2024;23(5):495–518. doi:10.1080/15384101.2024.2344943
11. Xiang P, Chen Q, Chen L, et al. Metabolite Neu5Ac triggers SLC3A2 degradation promoting vascular endothelial ferroptosis and aggravates atherosclerosis progression in ApoE(-/-)mice. *Theranostics*. 2023;13(14):4993–5016. doi:10.7150/thno.87968
12. Luo X, Wang Y, Zhu X, et al. MCL attenuates atherosclerosis by suppressing macrophage ferroptosis via targeting KEAP1/NRF2 interaction. *Redox Biol*. 2024;69:102987. doi:10.1016/j.redox.2023.102987
13. Shih CC, Chen CY, Chuu CP, et al. Transcriptome insights into protective mechanisms of ferroptosis inhibition in aortic dissection. *Int J Mol Sci*. 2025;26(9):4338. doi:10.3390/ijms26094338
14. Xu X, Xu XD, Ma MQ, et al. The mechanisms of ferroptosis and its role in atherosclerosis. *Biomed Pharmacother*. 2024;171:116112. doi:10.1016/j.biopha.2023.116112
15. Li C, Liu R, Xiong Z, et al. Ferroptosis: a potential target for the treatment of atherosclerosis. *Acta Biochim Biophys Sin*. 2024;56(3):331–344. doi:10.3724/abbs.2024016
16. Morgenstern C, Lastres-Becker I, Demirdöğen BC, et al. Biomarkers of NRF2 signalling: current status and future challenges. *Redox Biol*. 2024;72:103134. doi:10.1016/j.redox.2024.103134
17. Yamamoto M, Kensler TW, Motohashi H. The KEAP1-NRF2 system: a thiol-based sensor-effector apparatus for maintaining redox homeostasis. *Physiol Rev*. 2018;98(3):1169–1203. doi:10.1152/physrev.00023.2017
18. He L, Chen Q, Wang L, et al. Activation of Nrf2 inhibits atherosclerosis in ApoE(-/-) mice through suppressing endothelial cell inflammation and lipid peroxidation. *Redox Biol*. 2024;74:103229. doi:10.1016/j.redox.2024.103229
19. Dodson M, Castro-Portuguez R, Zhang DD. NRF2 plays a critical role in mitigating lipid peroxidation and ferroptosis. *Redox Biol*. 2019;23:101107. doi:10.1016/j.redox.2019.101107
20. Yu P, Su L, Li B, et al. Selenomethionine alleviates Aeromonas hydrophila-induced oxidative stress and ferroptosis via the Nrf2/HO1/GPX4 pathway in grass carp. *Fish Shellfish Immunol*. 2024;154:109927. doi:10.1016/j.fsi.2024.109927
21. Li D, Li X, Zhang X, et al. Geniposide for treating atherosclerotic cardiovascular disease: a systematic review on its biological characteristics, pharmacology, pharmacokinetics, and toxicology. *Chin Med*. 2024;19(1):111. doi:10.1186/s13020-024-00981-3
22. Wu M, Li X, Wang S, et al. Polydatin for treating atherosclerotic diseases: a functional and mechanistic overview. *Biomed Pharmacother*. 2020;128:110308. doi:10.1016/j.biopha.2020.110308
23. Zhang X, Wang Z, Li X, et al. Polydatin protects against atherosclerosis by activating autophagy and inhibiting pyroptosis mediated by the NLRP3 inflammasome. *J Ethnopharmacol*. 2023;309:116304. doi:10.1016/j.jep.2023.116304
24. Wu M, Liu M, Guo G, et al. Polydatin inhibits formation of macrophage-derived foam cells. *Evid Based Complement Alternat Med*. 2015;2015:729017. doi:10.1155/2015/729017
25. Wu M, Liu L, Xing Y, et al. Roles and mechanisms of hawthorn and its extracts on atherosclerosis: a review. *Front Pharmacol*. 2020;11:118. doi:10.3389/fphar.2020.00118
26. Wang SZ, Wu M, Chen KJ, et al. Hawthorn extract alleviates atherosclerosis through regulating inflammation and apoptosis related factors: an experimental study. *Chin J Integr Med*. 2019;25(2):108–115. doi:10.1007/s11655-018-3020-4
27. Wu M, Yang S, Liu G, et al. Treating unstable angina with detoxifying and blood-activating formulae: a randomized controlled trial. *J Ethnopharmacol*. 2021;281:114530. doi:10.1016/j.jep.2021.114530
28. Li D, Liu L, Yang S, et al. Exploring the therapeutic mechanisms of Huzhang-Shanzha herb pair against coronary heart disease by network pharmacology and molecular docking. *Evid Based Complement Alternat Med*. 2021;2021:5569666. doi:10.1155/2021/5569666
29. Ahmadi A, Argulian E, Leipsic J, et al. From Subclinical Atherosclerosis to Plaque Progression and Acute Coronary Events: JACC State-of-the-Art Review. *J Am Coll Cardiol*. 2019;74(12):1608–1617. doi:10.1016/j.jacc.2019.08.012
30. Maremonti F, Tonnus W, Gavali S, et al. Ferroptosis-based advanced therapies as treatment approaches for metabolic and cardiovascular diseases. *Cell Death Differ*. 2024;31(9):1104–1112. doi:10.1038/s41418-024-01350-1
31. Bai T, Li M, Liu Y, et al. Inhibition of ferroptosis alleviates atherosclerosis through attenuating lipid peroxidation and endothelial dysfunction in mouse aortic endothelial cell. *Free Radic Biol Med*. 2020;160:92–102. doi:10.1016/j.freeradbiomed.2020.07.026
32. Yang R, Gao W, Wang Z, et al. Polyphyllin I induced ferroptosis to suppress the progression of hepatocellular carcinoma through activation of the mitochondrial dysfunction via Nrf2/HO-1/GPX4 axis. *Phytomedicine*. 2024;122:155135. doi:10.1016/j.phymed.2023.155135
33. O'Rourke SA, Shanley LC, Dunne A. The Nrf2-HO-1 system and inflammaging. *Front Immunol*. 2024;15:1457010. doi:10.3389/fimmu.2024.1457010
34. Zhang Q, Liu J, Duan H, et al. Activation of Nrf2/HO-1 signaling: an important molecular mechanism of herbal medicine in the treatment of atherosclerosis via the protection of vascular endothelial cells from oxidative stress. *J Adv Res*. 2021;34:43–63. doi:10.1016/j.jare.2021.06.023
35. Rochette L, Dogon G, Rigal E, et al. Lipid peroxidation and iron metabolism: two corner stones in the homeostasis control of ferroptosis. *Int J Mol Sci*. 2022;24(1):449. doi:10.3390/ijms24010449
36. Dang R, Wang M, Li X, et al. Edaravone ameliorates depressive and anxiety-like behaviors via Sirt1/Nrf2/HO-1/Gpx4 pathway. *J Neuroinflammation*. 2022;19(1):41. doi:10.1186/s12974-022-02400-6
37. Gao Y, Wang B, Hu M, et al. The role of iron in atherosclerosis and its association with related diseases. *Curr Atheroscler Rep*. 2024;27(1):1. doi:10.1007/s11883-024-01251-1
38. Wang Y, Liao S, Pan Z, et al. Hydrogen sulfide alleviates particulate matter-induced emphysema and airway inflammation by suppressing ferroptosis. *Free Radic Biol Med*. 2022;186:1–16. doi:10.1016/j.freeradbiomed.2022.04.014
39. Zhu J, Dai X, Wang Y, et al. Molybdenum and cadmium co-induce apoptosis and ferroptosis through inhibiting Nrf2 signaling pathway in duck (Anas platyrhyncha) testes. *Poult Sci*. 2024;103(5):103653. doi:10.1016/j.psj.2024.103653
40. Wang X, Wang Y, Huang D, et al. Astragaloside IV regulates the ferroptosis signaling pathway via the Nrf2/SLC7A11/GPX4 axis to inhibit PM2.5-mediated lung injury in mice. *Int Immunopharmacol*. 2022;112:109186. doi:10.1016/j.intimp.2022.109186

41. Deng Y, Zeng L, Liu H, et al. Silibinin attenuates ferroptosis in acute kidney injury by targeting FTH1. *Redox Biol*. 2024;77:103360. doi:10.1016/j.redox.2024.103360
42. Li M, Meng Z, Yu S, et al. Baicalein ameliorates cerebral ischemia-reperfusion injury by inhibiting ferroptosis via regulating GPX4/ACSL4/ACSL3 axis. *Chem Biol Interact*. 2022;366:110137. doi:10.1016/j.cbi.2022.110137
43. Li D, Li Y, Yang S, et al. Polydatin combined with hawthorn flavonoids alleviate high fat diet induced atherosclerosis by remodeling the gut microbiota and glycolipid metabolism. *Front Pharmacol*. 2025;16:1515485. doi:10.3389/fphar.2025.1515485